PAPER

Check for updates

A diarylethene-based "on–off–on" fluorescence sensor for the sequential recognition of mercury and cysteine†

Gang Li, Lele Ma, Gang Liu,* Congbin Fan (ID) and Shouzhi Pu*

A novel photochromic diarylethene with a quinoline unit was synthesized with multi-controllable fluorescence switching properties, which could be induced by light, mercury (Hg^{2+}) and cysteine (Cys). Because the diarylethene displayed obvious fluorescence quenching with Hg^{2+} and the fluorescence was recovered to its original state evidently with Cys, it could sequentially recognize Hg^{2+} and Cys. Additionally, a logic circuit was constructed with the fluorescence intensity at 468 nm as output, and the combined stimuli of light and chemicals as inputs.

Introduction

As a hazardous chemical in the environment from a variety of natural and anthropogenic sources,[1,2] the mercury ion (Hg^{2+}) is a caustic and carcinogenic material with high cellular toxicity[3] because it accumulates in the human body and a very small amount can cause serious diseases, such as cardiovascular disease, serious cognitive and motion disorders, Minamata disease and coronary heart disease.[4–9] Therefore, monitoring Hg^{2+} in the environment has received increasing interest. Currently, various techniques and protocols, such as atomic absorption spectrometry, inductively coupled plasma, atomic emission spectroscopy, and capillary electrophoresis have been well developed and utilized to monitor Hg^{2+}.[10–13] However, most of these methods are still limited by complex instruments and complicated procedures with high cost, or low sensitivity and low selectivity. However, fluorescent sensors are very simple and sensitive in the detection of metal ions or harmful pollutants in the environment. Therefore, considerable efforts have been made to develop fluorescent molecular chemosensors for Hg^{2+}.[14–22]

As a small molecular weight biothiol, cysteine (Cys) plays a prominent role in various critical biological systems, such as metabolic processes, biocatalysis and detoxifications of xenobiotics.[23–27] However, Hg^{2+} ion can bond to Cys through Hg–S to cause many health problems,[28–30] such as slowed growth in children, liver damage, loss of muscle and fat, skin lesions and weakness.[31] On other hand, high levels of Cys in living systems also cause many human diseases, including developmental

retardation, cardiovascular, osteoporosis, Alzheimer's disease, *etc.*[32] Therefore, it is very important to detect Cys and Hg^{2+} in biological systems. Up to present, detection of Hg^{2+} and Cys was mainly based on photochromic materials with dual functionalities.[33–36] Among these various photochromic compounds, diarylethenes are one of the most promising photo-switchable molecules with excellent photochemical reactivity, thermal stability, fatigue resistance[37–40] and fluorescence.[41–43] For example, Tian and his co-workers have reported two photochromic diarylethene-based chemosensors with excellent optical properties to distinguish Hg^{2+} in acetonitrile.[44] We also synthesized a photochromic diarylethene with a formyl group. Because of the interaction between the formyl group of its ring-closed isomer with Cys, there was a notable change in its absorption spectrum with an evident color change from blue to pale yellow if Cys was added.[45] However, all of these reports were focused on recognizing Hg^{2+} and Cys individually.

In this study, we designed and synthesized a new photochromic diarylethene with a quinoline unit, which could sequentially recognize Hg^{2+} and Cys efficiently. Compared with previously reported results, this method was more feasible, economic, convenient and significant. The fluorescence of the diarylethene was quenched in the presence of Hg^{2+} in tetrahydrofuran. When a certain amount of Cys was subsequently added, the fluorescence was enhanced and restored to almost the intensity before quenching.

Experimental

General methods

NMR spectra were recorded on Bruker AV400 (400 MHz) spectrometer with $CDCl_3$ as the solvent and tetramethylsilane (TMS) as the internal standard. Mass spectra were measured on a Bruker AmaZon SL Ion Trap Mass spectrometer. IR spectra were recorded on a Bruker Vertex-70 spectrometer. Melting

Jiangxi Key Laboratory of Organic Chemistry, Jiangxi Science and Technology Normal University, Nanchang, Jiangxi 330013, PR China. E-mail: pushouzhi@tsinghua.org.cn; Fax: +86-791-83831996; Tel: +86-791-83831996

point was measured on a WRS-1B melting point apparatus. The absorption spectra were measured on an Agilent 8453 UV/Vis spectrophotometer. Photoirradiation was carried out with an SHG-200 UV lamp, CX-21 ultraviolet fluorescence analysis cabinet and a BMH-250 visible lamp. Light of appropriate wavelength was isolated through different light filters. Fluorescence spectra were recorded on a Hitachi F-4600 fluorescence spectrophotometer. The fluorescence quantum yield was measured on an Absolute PL Quantum Yield Spectrometer QY C11347-11. All inorganic salts ($Hg(ClO_4)_2 \cdot 6H_2O$, $Cd(NO_3)_2 \cdot 4H_2O$, $Zn(NO_3)_2 \cdot 6H_2O$, $Mg(NO_3)_2 \cdot 6H_2O$, $Ca(NO_3)_2 \cdot 4H_2O$, $Ba(NO_3)_2$, $Cr(NO_3)_3 \cdot 9H_2O$, $Al(NO_3)_3 \cdot 9H_2O$, $Ni(NO_3)_2 \cdot 6H_2O$, $MnCl_2 \cdot 4H_2O$, $Co(NO_3)_2 \cdot 6H_2O$, $Cu(NO_3)_2 \cdot 3H_2O$, $Sr(NO_3)_2$, $Pb(NO_3)_2$, $Fe(NO_3)_3 \cdot 9H_2O$ and KCl) and amino-acids (cysteine (Cys), glycine (Gly), alanine (Ala), valine (Val), leucine (Leu), isoleucine (Ile), phenylalanine (Phe), proline (Pro), tryptophan (Try), serine (Ser), tyrosine (Tyr), glutamine (Glu), threonine (Thr), glutamic acid (Glu), lysine (Lys), arginine (Arg), histidine (His)) were purchased and used without further purification. All metal ions and amino-acids were dissolved (0.1 mol L^{-1}) in distilled water. All other solvents used were of spectro-grade and purified through distillation prior to use.

Synthesis of 1O

The synthetic route of 1-(2-methyl-3-benzothiophenyl)-2-{2-methyl-5-(4-pheny)-(2-benzoylquinolines-8-benzothiazole)-3-thienyl}-perfluorocyclopentene (1O) was shown in Fig. 1. The intermediate 2 was synthesized according to literature.[46] Synthesis of 1-(2-methyl-3-benzothiophenyl)-2-{2-methyl-5-phenyl-4-(2-formylquinoline-8-methoxyl)-3-thienyl} perfluorocyclopentene (3).

To a compound 2 (0.58 g, 1.00 mmol) solution in anhydrous acetonitrile (30 mL), 8-hydroxyquinoline-2-carboxaldehyde (0.16 g, 0.90 mmol) and K_2CO_3 (0.33 g, 2.00 mmol) were added with continuously stirring. After 6 hours of refluxing, the mixture was cooled to room temperature and concentrated under vacuum. The crude product was purified through column chromatography on silica gel with petroleum ether/ethyl acetate (v/v = 6/1) as the eluent to afford compound 3 as a pale pink solid. The yield was 70%. Mp 340–342 K. ^{1}H NMR ($CDCl_3$, 400 MHz), δ (ppm) 1.93 (s, 3H), 2.30 (s, 3H), 5.47 (s, 2H), 7.15 (t, 2H, J = 8.0 Hz), 7.30–7.36 (m, 2H), 7.44–7.49 (m, 3H), 7.52–7.57 (m, 4H), 7.73 (d, 1H, J = 8.0 Hz), 8.08 (d, 1H, J = 8.4 Hz), 8.29 (d, 1H, J = 7.8 Hz), 10.33 (s, 1H).

Synthesis of 1-(2-methyl-3-benzothiophenyl)-2-{2-methyl-5-phenyl-4-(2-formylquinoline-8-benzothiazole)-3-thienyl} perfluorocyclopentene (1O).

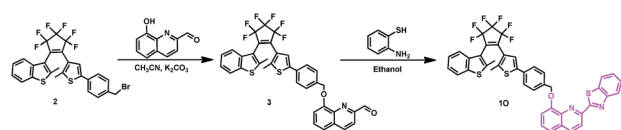Compound 3 (0.34 g, 0.5 mmol) and 2-aminothiophenol (0.06 g, 0.5 mmol) were dissolved in 5 mL of ethanol. After the

reaction mixture was refluxed for 6 hours, a light purple powder crude product appeared. Then, the reaction mixture was cooled to room temperature, washed with cold ethanol and dried in air. The yield was (0.31 g) 80%. Mp 438–440 K. ^{1}H NMR ($CDCl_3$, 400 MHz), δ (ppm) 1.93 (s, 3H), 2.31 (s, 3H), 5.46 (s, 2H), 7.13–7.21 (m, 1H), 7.24 (s, 1H), 7.30–7.40 (m, 3H), 7.47–7.51 (m, 2H), 7.53–7.59 (m, 4H), 7.67 (d, 2H, J = 8.0 Hz), 7.75 (d, 1H, J = 7.7 Hz), 8.02 (d, 1H, J = 7.7 Hz), 8.14 (d, 1H, J = 8.1 Hz), 8.30 (d, 1H, J = 8.5 Hz), 8.53 (d, 1H, J = 8.6 Hz). ^{13}C NMR ($CDCl_3$, 100 MHz), δ (ppm) 14.82, 14.89, 71.06, 112.08, 118.73, 120.35, 120.49, 122.06, 122.09, 122.13, 122.18, 122.57, 123.77, 124.51, 124.95, 125.19, 125.58, 125.73, 125.84, 126.27, 127.70, 127.92, 130.36, 132.78, 136.60, 136.97, 137.04, 138.22, 140.45, 141.58, 141.69, 142.49, 150.21, 154.46. ^{19}F NMR (DMSO, 376 MHz), δ (ppm) −130.15 (1F), −128.96 (1F), −108.29 (1F), −106.88 (1F), −106.36 (2F). (Fig. S1†) IR (KBr, ν, cm^{-1}): 522, 724, 839, 1052, 1190, 1272, 1379, 1447, 1561. (Fig. S2†) LRMS: m/z 807.0 [M + Na]$^{+}$.

Results and discussion

Photochromism and fluorescence of 1O

The photochromic and fluorescent behaviors of 1O were studied in THF solution (2.0 × 10^{-5} mol L^{-1}) at room temperature, its absorption spectral, fluorescence spectral and color changes were induced by alternating irradiation with 297 nm UV light and visible light (λ > 500 nm) (Fig. 2). As shown in Fig. 2A, the absorption maximum of 1O was at 298 nm due to its π–π* transition.[47,48] Upon the irradiation with 297 nm UV light, a new absorption band centered at 548 nm emerged due to the formation of the closed-ring isomer 1C of 1O with larger π-electron delocalization in the molecule, which was accompanied with a color change from colorless to purple. After 5 minutes of irradiation with 297 nm UV light, the photocyclization reaction reached a photostationary state (PSS), and the photoconversion ratio from the openring isomer 1O to the closed-ring isomer 1C was 84% based on the HPLC analysis. (Fig. S3†) The cyclization and cycloreversion quantum yield of the diarylethene were 0.34 and 0.027, respectively, with 1,2-bis(2-methyl-5-phenyl-3-thienyl)-perfluorocyclopentene as the reference.[49] Reversely, the absorption spectrum of 1C with purple solution could be completely bleached to the initial state of 1O upon the visible light irradiation (λ > 500 nm). Fig. 2B showed the emission spectral changes of 1O upon

Fig. 1 Synthetic route for 1O.

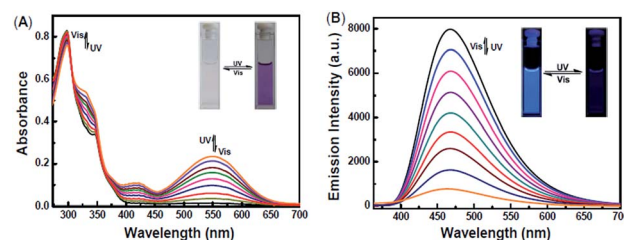

Fig. 2 Changes in the absorption and fluorescence of 1O upon alternating irradiation with UV and visible light in THF: (A) absorption spectra change (2.0 × 10^{-5} mol L^{-1}); (B) fluorescence change (2.0 × 10^{-5} mol L^{-1}), excited at 354 nm.

photoirradiation when excited at 354 nm. Upon irradiation with 297 nm UV light, the emission peak of **1O** was decreased significantly due to the formation of non-fluorescent closed-ring isomer **1C**, which was accompanied by an obvious fluorescence intensity change from light blue to dark. In the photostationary state, the emission intensity of **1O** was quenched to *ca.* 97%, and the fluorescence quantum yield of **1O** to **1C** was determined to be 0.459 to 0.008. Similarly, the fluorescence intensity of **1** could also be recovered with the irradiation of appropriate visible light ($\lambda > 500$ nm).

Fluorescent turn-off detection of Hg^{2+}

The fluorescence response of **1O** toward 16 different metal ions (Hg^{2+}, Cd^{2+}, Zn^{2+}, Mg^{2+}, Ca^{2+}, Ba^{2+}, Cr^{3+}, Al^{3+}, Ni^{2+}, Mn^{2+}, Co^{2+}, Cu^{2+}, Sr^{2+}, Pb^{2+}, Fe^{3+}, K^+) was measured in THF (2.0×10^{-5} mol L^{-1}) at room temperature. As shown in Fig. 3A, diarylethene **1O** displayed a strong fluorescence with an emission of 468 nm. The addition of 5.0 equiv. metal ion (Cd^{2+}, Zn^{2+}, Mg^{2+}, Ca^{2+}, Ba^{2+}, Cr^{3+}, Al^{3+}, Ni^{2+}, Mn^{2+}, Co^{2+}, Cu^{2+}, Sr^{2+}, Pb^{2+} or K^+) to the solution, **1O** showed no significant changes in its fluorescence, while the same amount of Fe^{3+} caused the fluorescence intensity to decrease by almost 30%. The addition of Hg^{2+} into **1O** resulted in the complete quench of its fluorescence intensity. The Fig. 3B shows the fluorescence color changes of **1O** when the various metal ions added. These results indicated that **1O** could easily discriminate Hg^{2+} from others metal ions.

As shown in Fig. 4, when the **1O** was titrated with Hg^{2+}, the fluorescence intensity was significantly decreased until 3.2 equiv. of Hg^{2+} were added. With further addition of Hg^{2+}, the fluorescence intensity was then decreased slowly. When 5.0 equiv. of Hg^{2+} were added, the fluorescence intensity of **1O** was almost quenched completely. The quantum yields of **1O′** (the complex of **1O** added the Hg^{2+}) from 0.459 to 0.11 were determined. Meanwhile, based on the linear Benesi–Hildebrand expression and the Stern–Volmer plot, linear relationships
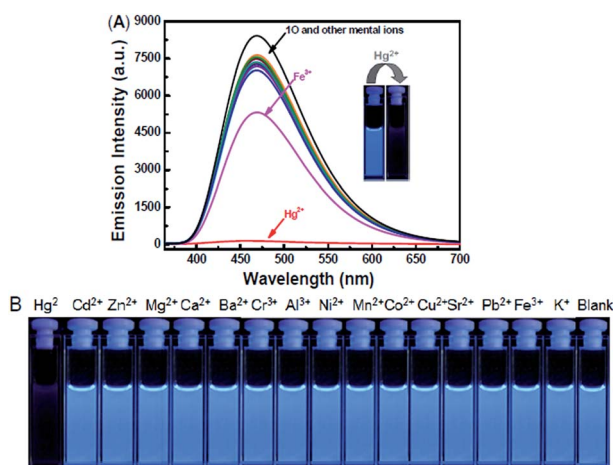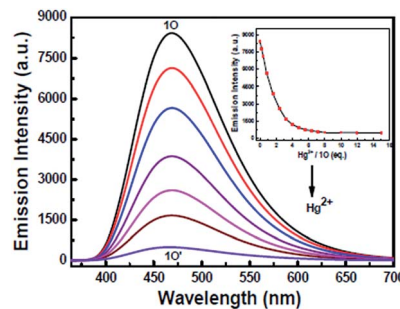
Fig. 4 Changes in the fluorescence of **1O** induced by Hg^{2+} in THF (2.0×10^{-5} mol L^{-1}) and emission intensity changes of **1O** induced by the addition of different equiv. of Hg^{2+}.

between **1O′** fluorescence at 468 nm and **1O**/[Hg^{2+}] were obtained. The association constant of Hg^{2+} binding to diarylethene **1O** was found as 1.11×10^4 L mol^{-1} ($R = 0.99858$). The limit of **1O** as a fluorescent sensor to detect Hg^{2+} was 4.76×10^{-8} mol L^{-1}, which was determined from a plot of intensity as a function of the concentration of Hg^{2+} (Fig. S4†).[50]

Comparative, Job's plots and the ESI-MS experiments were conducted to elucidate the binding mode of **1O** with Hg^{2+}. The naphthol-benzothiazole moiety (**NBTZ**), quinolinol-benzoxazole moiety (**QBOZ**) and quinolinol-benzothiazole (**QBTZ**) moiety were synthesized to the comparative experiments and all the ^1H NMR, ^{13}C NMR datas were conducted. (Fig. S5†) Then, the detection to Hg^{2+} in THF (2.0×10^{-5} mol L^{-1}) of the precursor **3**, **NBTZ**, **QBOZ** and **QBTZ** were tested. The precursor **3** and the probe **NBTZ** have no effect on Hg^{2+}, the probe **QBOZ** and **QBTZ** could all be quenched by Hg^{2+}. (Fig. S6†) These phenomenon indicated that the Hg^{2+} could combine the atom "N" from the quinoline, the other bridging site could not be determined. While, the same structure that contains quinolinol-benzimidazole in our earlier published paper that could not recognize Hg^{2+}.[51] So, we think the other possible bridging site was the atom "S" from the benzothiazole. According to its ESI-MS spectrometry of **1O′** (Fig. S7†), it had a 1 : 1 complexation stoichiometry in $1O - Hg^{2+}$ complex with a peak at m/z 985.3 due to $[1O + Hg^{2+}]^+$, another peak at m/z 1209.9 due to $[1O + Hg^{2+} + 2ClO_4^- + Na^+]^+$. As shown in Fig. 5 of Job's plots, the maximum value was achieved when the molar fraction of $[Hg^{2+}]/([Hg^{2+}] + [1O])$ was about 0.5, which further demonstrated the 1 : 1 stoichiometry between **1O** with Hg^{2+}.

Fig. 3 Competitive changes in the fluorescence of **1O** in THF (2.0×10^{-5} mol L^{-1}) with the addition of various metal ions (5.0 equiv.): (A) emission spectral changes, (B) image of the fluorescence color changes.
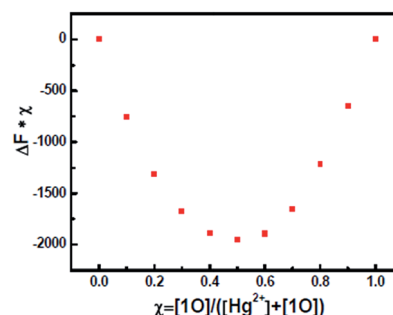
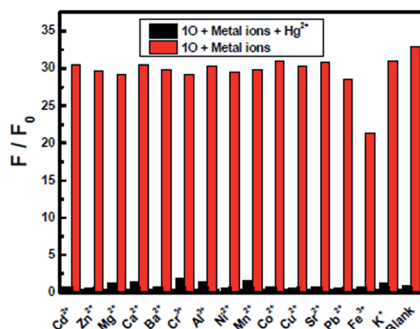**Fig. 5** Job's plot of **1O** with Hg^{2+}.

Fig. 6 Competitively fluorescent response tests of **1O′** to various metal ions in THF (2.0×10^{-5} mol L^{-1}). Red bars represent the addition of 5.0 equiv. of various metal ions to the solution of **1O**. Black bars represent the addition of Hg^{2+} (5.0 equiv.) to the above solution, respectively.

In the competitive experiment, the fluorescence quenching of diarylethene **1O** caused by 5.0 equiv. of Hg^{2+} was retained in the presence of the same concentration of other metal ions, including Cd^{2+}, Zn^{2+}, Mg^{2+}, Ca^{2+}, Ba^{2+}, Cr^{3+}, Al^{3+}, Ni^{2+}, Mn^{2+}, Co^{2+}, Cu^{2+}, Sr^{2+}, Pb^{2+}, Fe^{3+} and K^{+}. These results indicated that **1O** had an excellent selectivity to Hg^{2+} over other metal ions (Fig. 6).

Fluorescent turn-on response of 1O′ toward Cys

As shown in Fig. 7, studies on **1O′** fluorescent spectra with 17 different amino-acids, such as Cys, Gly, Ala, Val, Leu, Ile, Phe, Pro, Try, Ser, Tyr, Glu, Thr, Glu, Lys and Arg were conducted in THF. Becasue Hg^{2+} has high affinity towards thiol-based amino-acids,[52–54] the fluorescence intensity of **1O′** almost recovered to the original of **1O** only when Cys was added into the solution, and the quantum yields of **1O′** + Cys was measured as 0.426, while other amino-acids did not change the emission spectra. The fluorescence recovery might be due to release of **1O** from the **1O′** through the interaction of thiol-containing Cys with Hg^{2+}. Then, others organic thiol compounds like ethylene mercaptan, 2-aminothiophenol and 2-aminoethanethiol were
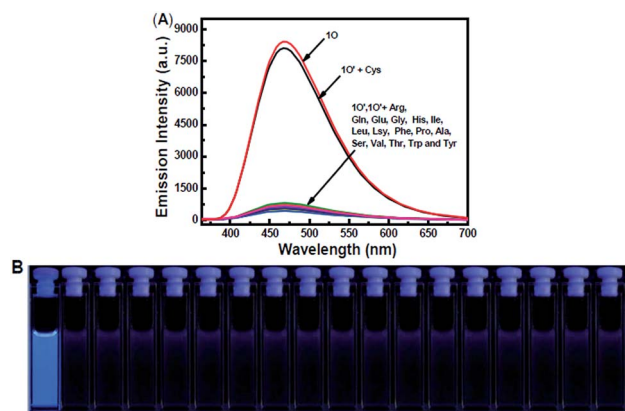
tested and the fluorescence could also recovery. (Fig. S8†) These results showed that **1O′** could be successfully utilized to sensor thiol-containing compounds with turn-on fluorescence.

As shown in Fig. 8, when Cys was added to the solution of **1O′**, the fluorescence of the solution was enhanced rapidly. When 5.0 equiv. of Cys was added, the fluorescence recovered to the original of **1O**, indicating that Cys took the Hg^{2+} away from **1O′**. According to the Job's plots (Fig. 9) and ESI-MS spectrometry (Fig. S9†), the complex **1O′** − Cys had a 1 : 2 coordination stoichiometry. In the negative-ion mass spectrum, the peak at m/z 441.4 was assignable to [2Cys + Hg^{2+} + H]$^{-}$ and the other peak at m/z 785 was assignable to **1O**. Similarly, according to Benesi–Hildebrand, the binding constant between **1O′** and Cys was 7.86×10^{3} L mol^{-1} ($R = 0.99351$) and the detection limit of **1O′** was 7.06×10^{-8} mol L^{-1} (Fig. S10†).

As shown in Fig. 10, when **1O′** was treated with 5.0 equiv. of Cys in the presence of the same concentration of other amino-acids, the emission enhancement caused by Cys was retained with Gly, Ala, Val, Leu, Ile, Phe, Pro, Try, Ser, Tyr, Glu, Thr, Glu, Lys, Arg and His, which indicated that any other amino acids could not interference the detection of Cys by **1O′** in THF.

Application of 1O in logic circuits

Since the fluorescence intensity of **1O** could be controlled by the stimulation of UV/Vis light, Hg^{2+} and Cys, a combinational logic circuit could be constructed with four inputs (In1: 297 nm UV

Fig. 8 Fluorescence changes of **1O′** induced by Cys in THF (2.0×10^{-5} mol L^{-1}) and emission intensity changes of **1O′** induced by different equiv. of Cys.

Fig. 7 Changes in fluorescence of **1O′** induced by Cys in THF (2.0×10^{-5} mol L^{-1}): (A) emission spectral changes; (B) image demonstrating changes in fluorescence.
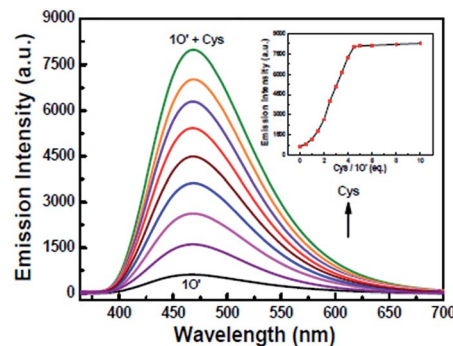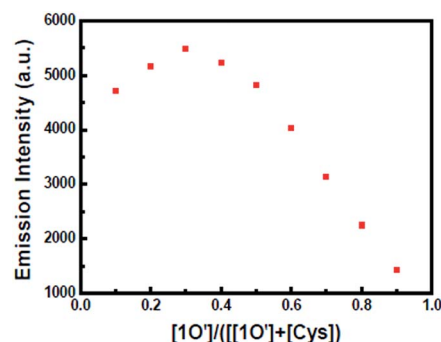

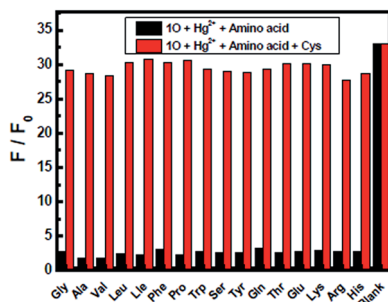**Fig. 9** Job's plot of **1O′** with Cys.

Fig. 10 Competitive tests on the fluorescent responses of **1O′** + Cys to various amino acids in THF (2.0×10^{-5} mol L^{-1}). Black bars represent the addition of 5.0 equiv. of various amino acids to the **1O′** solution. Red bars represent the addition of Cys (5.0 equiv.) to the above solution, respectively.
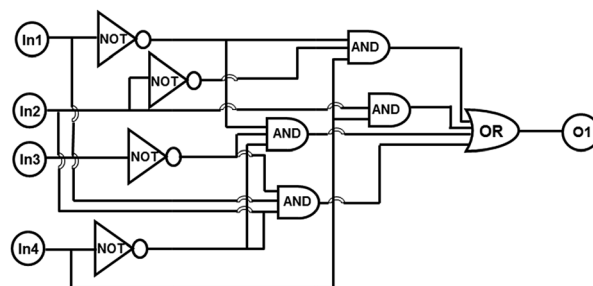

Fig. 11 Combinational logic circuits equivalent to the truth table given in Table 1: In1 (UV), In2 (Vis), In3 (Hg^{2+}), In4 (Cys).

light, In2: $\lambda > 500$ nm visible light, In3: Hg^{2+} and In4: Cys) and one output signal (the change of fluorescence intensity at 468 nm). The emission intensity of **1O** at 468 nm was regarded as the initial value.

All the four inputs could be either "on" or "off" state with different Boolean values. When the emission intensity was quenched by over 50% of the initial value, the output signal could be regarded as 'off' state with a Boolean value of '0'. Otherwise, it was regarded as 'on' state with a Boolean value of '1'. The diarylethene **1O** showed an on–off–on fluorescence switching behavior under the stimuli of different inputs. For example, when the string is '0, 0, 1, and 0' the corresponding input signals of In1, In2, In3, and In4 are 'off, off, on, off'. It means that **1O** was stimulated by Hg^{2+} and its emission intensity quenched dramatically. And the output signal was 'off' with a digit of '0'. All possible strings of the three inputs were listed in Table 1 and the logic circuit corresponding to the truth table was shown in Fig. 11.

Conclusions

In summary, a new diarylethene-based "on–off–on" fluorescence sensor for the sequential recognition of Hg^{2+} and Cys with very high selectivity and sensitivity was designed and synthesized successfully. When Hg^{2+} was added into the solution of **1O**, fluorescence of the **1O** solution was quenched because **1O** bond to Hg^{2+} into $[\mathbf{1O} - \text{Hg}^{2+}]$ (**1O′**) 1 : 1 stoichiometry. When Cys was added into **1O′** solution, the fluorescence was enhanced significantly due to the reaction between **1O′** and Cys in 1 : 2 stoichiometry. Based on the fact that the fluorescence of the diarylethene could be effectively modulated with the stimulation of light and chemical species, a logic circuit was also constructed successfully with the fluorescence intensity as the output signal, and UV/Vis, Hg^{2+} and Cys as the inputs, which should have great potentials in future fluorescent sensors for some special species.

Acknowledgements

Notes and references

1 H. N. Kim, W. X. Ren, J. S Kim and J. Yoon, *Chem. Soc. Rev.*, 2012, **41**, 3210–3244.
2 M. Li, X. J. Zhou, W. Q. Ding, S. W. Guo and N. Q. Wu, *Biosens. Bioelectron.*, 2013, **79**, 889–893.
3 N. Zheng, Q. C. Wang, X. W. Zhang, D. M. Zheng, Z. S. Zhang and S. Q. Zhang, *Sci. Total Environ.*, 2007, **387**, 96–104.
4 J. K. Virtanen, T. H. Rissanen, S. Voutilainen and T. P. Tuomainen, *J. Nutr. Biochem.*, 2007, **18**, 75–85.
5 T. W. Clarkson, L. Magos and G. J. Myers, *N. Engl. J. Med.*, 2003, **349**, 1731–1737.
6 J. Gutknecht, *J. Membr. Biol.*, 1981, **61**, 61–66.
7 E. M. Nolan and S. J. Lippard, *Chem. Rev.*, 2008, **108**, 3443–3480.

Table 1 Truth table for all possible strings of the four binary-input data and the corresponding output digit

Input				Output^a λ_{em} = 468 nm
In1 (UV)	In2 (Vis)	In3 (Hg^{2+})	In4 (Cys)	
0	0	0	0	1
1	0	0	0	0
0	1	0	0	1
0	0	1	0	0
0	0	0	1	1
1	1	0	0	1
1	0	1	0	0
1	0	0	1	0
0	1	1	0	0
0	1	0	1	1
0	0	1	1	1
1	1	1	0	0
1	1	0	1	1
1	0	1	1	0
0	1	1	1	1
1	1	1	1	1

^{a} The emission intensity of **1O** at 468 nm was regarded as the initial value and defined as 1, otherwise defined as 0.

8 Y. W. Chen, C. F. Huang, K. S. Tsai, R. S. Yang, C. C. Yen, C. Y. Yang, S. Y. Lin-Shiau and S. H. Liu, *Chem. Res. Toxicol.*, 2006, **19**, 1080–1085.

9 P. Holmes, K. A. F. James and L. S. Levy, *Sci. Total Environ.*, 2009, **408**, 171–182.

10 M. Ghaedi, M. R. Fathi, A. Shokrollahi and F. Shajarat, *Anal. Lett.*, 2006, **39**, 1171–1185.

11 T. Matousek, A. Z. Hernández, M. Svoboda, L. Langrová, B. M. Adair, Z. Drobná, D. J. Thomas, M. Styblo and J. Dedina, *Spectrochim. Acta, Part B*, 2008, **63**, 396–406.

12 X. Y. Jia, Y. Han, X. L. Liu, T. C. Duan and H. T. Chen, *Spectrochim. Acta, Part B*, 2011, **66**, 88–92.

13 Y. L. Feng, H. W. Chen and H. Y. Chen, *J. Anal. Chem.*, 1998, **361**, 155–157.

14 B. Han, J. Yuan and E. Wang, *Anal. Chem.*, 2009, **81**, 5569–5573.

15 B. Cao, C. Yuan, B. Liu, C. Jiang, G. Guan and M. Y. Han, *Anal. Chim. Acta*, 2013, **786**, 146–152.

16 C. Wang, D. Zhang, X. Huang, P. Ding, Z. Wang, Y. Zhao and Y. Ye, *Sens. Actuators, B*, 2014, **198**, 33–40.

17 D. H. Kim, J. Seong, H. Lee and K. H. Lee, *Sens. Actuators, B*, 2014, **196**, 421–428.

18 M. Li, Q. Wang, X. Shi, L. A. Hornak and N. Wu, *Anal. Chem.*, 2011, **83**, 7061–7065.

19 R. M. Kong, X. B. Zhang, L. L. Zhang, X. Y. Jin, S. Y. Huan, G. L. Shen and R. Q. Yu, *Chem. Commun.*, 2009, 5633–5635.

20 M. Hollenstein, C. Hipolito, C. Lam, D. Dietrich and D. M. Perrin, *Angew. Chem., Int. Ed.*, 2008, **47**, 4346–4350.

21 H. Urata, E. Yamaguchi, T. Funai, Y. Matsumura and S. I. Wada, *Angew. Chem.*, 2010, **122**, 6666–6669.

22 Y. Zhao and Z. Zhong, *J. Am. Chem. Soc.*, 2006, **128**, 9988–9989.

23 S. Seshadri, A. Beiser, J. P. Selhub, F. I. Jacques, H. Rosenberg, R. B. D. Agostino, P. W. Wilson and P. A. N. Wolf, *N. Engl. J. Med.*, 2002, **346**, 476–483.

24 S. A. Lee, J. J. Lee, J. W. Shin, K. S. Min and C. Kim, *Dyes Pigm.*, 2015, **116**, 131–138.

25 Y. Yang, F. J. Huo, C. Yin, J. Chao and Y. Zhang, *Dyes Pigm.*, 2015, **114**, 105–109.

26 C. Hwang, A. J. Sinskey and H. F. Lodish, *Science*, 1992, **257**, 1496–1502.

27 L. Wang, Q. Zhou, B. Zhu, L. Yan, Z. Ma, B. Du and X. Zhang, *Dyes Pigm.*, 2012, **95**, 275–279.

28 F. Jalilehvand, B. O. Leung, M. Izadifard and E. Damian, *Inorg. Chem.*, 2006, **45**, 66–73.

29 J. S. Wu, R. L. Sheng, W. M. Liu, P. F. Wang, J. J. Ma, H. Y. Zhang and X. Q. Zhuang, *Inorg. Chem.*, 2011, **50**, 6543–6551.

30 G. Mcdonnell and D. A. Russell, *Clin. Microbiol. Rev.*, 1999, **12**, 147–157.

31 S. Shahrokhian, *Anal. Chem.*, 2001, **73**, 5972–5978.

32 C. Jacob, G. I. Giles, N. M. Giles and H. Sies, *Angew. Chem., Int. Ed.*, 2003, **42**, 4742–4758.

33 Z. Li, Y. Wang, Y. N. Ni and S. Kokot, *Sens. Actuators, B*, 2015, **207**, 490–497.

34 B. L. Feringa, *Molecular Switches*, 2001.

35 V. Balzani, M. Venturi and A. Cred, *Molecular Devices and Machines*, 2003.

36 I. Willner, *Acc. Chem. Res.*, 1997, **30**, 347–356.

37 K. Higashiguchi, K. Matsuda, N. Tanifuji and M. Irie, *J. Am. Chem. Soc.*, 2005, **127**, 8922–8923.

38 B. M. Neilson and C. W. Bielawski, *J. Am. Chem. Soc.*, 2012, **134**, 12693–12699.

39 S. Kawata and Y. Kawata, *Chem. Rev.*, 2000, **100**, 1777–1788.

40 Y. Nakayama, K. Hayashi and M. Irie, *J. Org. Chem.*, 1990, **55**, 2592–2596.

41 F. Duan, G. Liu, P. Liu, C. B. Fan and S. Z. Pu, *Tetrahedron*, 2016, **72**, 3213–3220.

42 S. J. Xia, G. Liu and S. Z. Pu, *J. Mater. Chem. C*, 2015, **3**, 4023.

43 S. Q. Cui, Z. Y. Tian, S. Z. Pu and Y. F. Dai, *RSC Adv.*, 2016, **6**, 19957.

44 Q. Zou, J. Y. Jin, B. Xu, L. Ding and H. Tian, *Tetrahedron*, 2011, **67**, 915–921.

45 C. H. Zheng, S. Z. Pu, G. Liu, B. Chen and Y. F. Dai, *Dyes Pigm.*, 2013, **98**, 280–285.

46 S. Z. Pu, L. L. Ma, G. Liu, H. C. Ding and B. Chen, *Dyes Pigm.*, 2015, **113**, 70–77.

47 Z. X. Li, L. Y. Liao, W. Sun, C. H. Xu, C. Zhang, C. J. Fang and C. H. Yan, *J. Mater. Chem. C*, 2008, **112**, 5190–5196.

48 L. Yuan, W. Y. Lin, Z. M. Cao, J. L. Wang and B. Chen, *Chem.–Eur. J.*, 2012, **18**, 1247–1255.

49 M. Irie, T. Lifka, S. Kobatake and N. Kato, *J. Am. Chem. Soc.*, 2000, **122**, 4871–4876.

50 S. Y. Tao, Y. Wei, C. Wang and B. J. Ding, *RSC Adv.*, 2014, **4**, 46955–46961.

51 G. Li, G. Liu, D. B. Zhang and S. Z. Pu, *Tetrahedron*, 2016, **72**, 6390–6396.

52 Y. Y. Fu, H. X. Li, W. P. Hu and D. B. Zhu, *Chem. Commun.*, 2005, 3189–3191.

53 N. Shao, J. Y. Jin, S. M. Cheung and R. H. Yang, *Angew. Chem., Int. Ed.*, 2006, **45**, 4944–4948.

54 Z. Q, Guo, S. W. Nam, S. S. Park and J. Y. Yoon, *Chem. Sci.*, 2012, **3**, 2760–2765.

This journal is © The Royal Society of Chemistry 2017